DUCTILE SEISMIC RETROFIT OF STEEL DECK-TRUSS BRIDGES. II: DESIGN APPLICATIONS

By Majid Sarraf[1] and Michel Bruneau,[2] Members, ASCE

ABSTRACT: A companion paper has demonstrated how deck-truss bridges can be retrofitted by converting the end cross-frames and lower end panels adjacent to the truss supports into special ductile panels. However, the design of such retrofitted systems must respect constraints on flexibilities to limit global drifts and ductility demands, as well as other constraints germane to the type of ductile device introduced. Proposed, here, are performance based design procedures accompanied by graphical approaches that incorporate all of those constraints affecting seismic response of deck-truss bridges retrofitted using eccentrically braced frames, vertical shear links, or triangular-plate added damping and stiffness device ductile systems. Using the proposed method, ductile panels for a 80-m-span deck-truss example bridge using eccentrically braced frames, vertical shear links, and triangular-plate added damping and stiffness device were designed, detailed, and modeled by computer. From the results of nonlinear inelastic time history analyses of the retrofitted bridge, it is concluded that all three systems designed according to the proposed procedure perform satisfactorily and enhanced seismic performance of the deck-truss bridges.

INTRODUCTION

A companion paper (Sarraf and Bruneau 1998) proposed a seismic retrofit strategy for deck-truss bridges that required conversion of the end cross-frames and the lower end panels adjacent to the truss supports, into special ductile panels acting as structural fuses. In accordance with capacity-design principles, the yield strength of these ductile panels must be chosen to limit the force demand in the superstructure and substructure, thus allowing damage to only occur in the specially detailed structural fuses in a controlled manner. Many structural systems or ductile devices can be used to provide the ductile panels, such as vertical shear links (VSL), triangular-plate added damping and stiffness device (TADAS) systems, and eccentrically braced frames (EBF), to name a few. These systems provide energy dissipation by ductile yielding of structural steel and have been used effectively in many building applications (Roeder and Popov 1977; Fehling et al. 1992; Tsai et al. 1993; Bouwkamp et al. 1994; Nakashima 1994). However, they have never been implemented in bridges.

In building applications, EBF and VSL can be designed using a simple codified procedure; TADAS systems have been used primarily to provide added damping for drift control in existing buildings. Although one could initially expect that simple design rules are possible for the deck-truss retrofit application of interest here, the first design attempts immediately reveal that complications exist due to the large number of strength, drift, and ductility demand limits that must be respected to achieve the design objectives. Seismic load paths and hierarchy of yielding in deck-truss bridges also differ from what is assumed in multistory frames. Systematic design procedures that recognize the aforementioned conditions are thus necessary and are presented in this paper. Note that additional constraints germane to each ductile system or device must always be considered, and this is illustrated by consideration of EBF, VSL, and TADAS systems in this paper. A seismic retrofit design example is provided for each system as implemented in the 80-m-span deck-truss considered by Sarraf and Bruneau (1998).

Note that solutions that respect all constraints are not always possible, and it is found that some types of ductile systems are considerably simpler to design and are more suitable for this application. In all cases, simpler solutions are obviously possible if the engineer is willing to violate some of the constraints considered here. Also note that the work presented here is valid as long as the limits and assumptions presented in Sarraf and Bruneau (1998) are respected.

GENERAL CONSTRAINTS FOR DESIGN OF DUCTILE PANELS

To achieve the desired seismic performance, the ductile panels must be designed with adequate strength and stiffness to satisfy global ductility and displacements limits, respectively. In particular, regardless of the type of ductile retrofit system, the fundamental period of the deck-truss T shall satisfy

$$T_{\min} \leq T \leq T_{\max} \tag{1}$$

where $T_{\min}$ and $T_{\max}$ are determined based on global ductility capacity and drift limits. In the companion paper, this inequality was expanded in terms of stiffnesses. However, in the design perspective presented here, constraints on flexibilities are more convenient. Therefore, the last few equations presented in the companion paper can be recast as follows. Limits on global flexibility f_{Global} can be expressed as

$$\frac{T_{\min}^2}{4\pi^2 M} \leq f_{\text{Global}} \leq \frac{T_{\max}^2}{4\pi^2 M} \tag{2}$$

Then, taking $f_{\min} = \alpha T_{\min}^2/4\pi^2 M$ and $f_{\max} = \alpha T_{\max}^2/4\pi^2 M$, where α = ratio of end panel flexibility $f_{E,S}$ to global flexibility f_{Global}, limits on flexibility of the retrofitted end panel $f_{E,S}$ becomes

$$f_{\min} \leq f_{E,S} \leq f_{\max} \tag{3}$$

Here, α can be taken as $2 \times (1 + R_{L,E}/R_{E,S}) = 2 \times (1 + f_{E,S}/f_{L,E})$ to favor simultaneous yielding of both end and lower end panels (Sarraf and Bruneau 1998), in which $R_{L,S}$ is the yield capacity of the lower end panel, $R_{E,S}$ is the yield capacity of the end panel, and $f_{L,E}$ is the flexibility of the lower end panel.

Another lower bound for flexibility is given by consideration of the entire lower path system, which can be modeled as two springs in series, and is expressed as

$$f_{L,S} = f_{L,E} + f^* \tag{4}$$

or

[1]PhD Candidate/Lect., Ottawa-Carleton Earthquake Engrg. Res. Ctr., Dept. of Civ. Engrg., Univ. of Ottawa, Ottawa, Ontario, Canada K1N 6N5. E-mail: msarraf@uottawa.ca

[2]Prof. and Dir., Ottawa-Carleton Earthquake Engrg. Res. Ctr., Dept. of Civ. Engrg., Univ. of Ottawa, Ottawa, Ontario, Canada K1N 6N5.

Note. Associate Editor: Sashi K. Kunnath. Discussion open until April 1, 1999. Separate discussions should be submitted for the individual papers in this symposium. To extend the closing date one month, a written request must be filed with the ASCE Manager of Journals. The manuscript for this paper was submitted for review and possible publication on February 18, 1998. This paper is part of the ***Journal of Structural Engineering***, Vol. 124, No. 11, November, 1998. ©ASCE, ISSN 0733-9445/98/0011-1263–1271/$8.00 + $.50 per page. Paper No. 17813.

$$f_{L,E} = f_{L,S} - f^* \tag{5}$$

where f^* = generalized flexibility of the lower lateral sway-frame subsystem. Obviously, the value of $f_{L,E}$ must be greater than zero, and thus, $f_{L,S} \geq f^*$. From the preceding definition of α, one can directly obtain

$$f_{L,S} = \frac{2}{\alpha - 2} f_{E,S} \tag{6}$$

Combining the inequality $f_{L,S} \geq f^*$ and (6), a limit for $f_{E,S}$ is given by

$$f_{E,S} \geq f^* \frac{\alpha - 2}{2} \tag{7}$$

Therefore, both (3) and (7) must be considered to select the flexibility of the end panel retrofit system. Once an appropriate value for the end panel flexibility $f_{E,S}$ is selected, the lower end retrofit panel flexibility can be determined by back-substituting values in (6), (7), and (5).

Note that a suitable value for $f_{E,S}$ must be selected by also taking into account all case specific design requirements for the chosen ductile system in addition to the limits given in (3) or (7). A systematic procedure to design ductile panels is possible when flexibility of the panels is expanded in terms of the geometry and size of the members to be designed. The following sections describes how this can be done for three specific types of ductile systems having their own special physical characteristics.

DESIGN OF EBF DUCTILE PANELS

Flexibility of EBF

Flexibility of an eccentrically braced end panel $f_{E,S}$ can be expressed as

$$f_{E,S} = \frac{h^2}{2Elb}\left[\frac{(a+e)^2}{3} - \frac{(b^2 - 2a^2)}{6}\right] + \frac{(a^2 + h^2)^{3/2}}{2EA_b a^2} + \frac{h^3}{2EA_{col}a^2} + \frac{(b-e)}{4EA_l} + \frac{eh^2}{2GA_S ab} \tag{8}$$

where $a = (b - e)/2$; b = panel width; h = height; A_{col} = cross-sectional area of a vertical panel member; A_b = cross-sectional area of a bracing member; A_l, A_S, and I = the cross-sectional area, shear area, and moment of inertia of the link beam, respectively; and e = link length.

In a seismic retrofit perspective, the parameters h and b are given. A_{col} is also a known value because it is assumed in this study that strengthening of the vertical members of the ductile panel is not a desirable action. For a given panel size and lateral force acting on the panel, A_b can be determined using an assumed panel geometry (i.e., link length and brace angle); link length must be determined by the design process, but the force in bracing members do not vary significantly with changes in value of e within practical limits. Note that, in accordance with capacity design principles, braces must be designed with a safety margin against buckling or yielding.

For an eccentric link yielding in shear, the needed shear area A_S must be equal to

$$A_S = \frac{R}{0.58F_y} \times \frac{h}{b} \tag{9}$$

in which, the term $0.58F_y$ is in fact the shear yielding stress, and R is the yield capacity of the panel.

Variations in the moment of inertia and length of the link beam have a significant impact on the flexibility and behavior of the panel and are, therefore, the critical design parameters.

Consequently, it is useful to rearrange (8) into

$$I = \frac{\frac{h^2}{2b}\left[\frac{(a+e)^2}{3} - \frac{(b^2 - 2a^2)}{6}\right]}{Ef_{E,S} - \frac{(a^2 + h^2)^{3/2}}{2A_b a^2} - \frac{h^3}{2A_{col}a^2} - \frac{(b-e)}{4A_l} - \frac{Eeh^2}{2GA_S ab}} \tag{10}$$

which can be used to determine the link beam inertia I necessary to provide the desirable end panel flexibility $f_{E,S}$ [defined by (3)], for a given link length e (9).

For a I-shaped link beam, beam depth d can also be expressed in terms of this moment of inertia through the following equation:

$$d = \sqrt{\frac{12I}{6A_f + A_S}} \tag{11}$$

where A_f and A_S = link beam's flange and web areas, respectively; and I depends on e as in (10). In other words, limits on flexibility of the end panel can also be related to depth of the link beam. The value of A_f is not readily available, but to start the design process an initial value can be selected using a A_f/A_S ratio reasonable for wide-flange beams and considering width-to-thickness ratio limit of the beam flange.

Proposed Design Procedure

To make the design process more systematic and manageable given the large number of constraints, a procedure is proposed in which all design requirements are expressed in the form of a set of inequalities with respect to a pair of design parameters. For EBF, depth of the link beam d and link length e are the preferred parameters. A graphical approach is proposed to define the range of admissible designs, because each design constraint can be plotted as a boundary line relating d to e.

The first two design constraints are obtained from (10) and (11). Equations for $d_1 = d(I_{max}, e)$ and $d_2 = d(I_{min}, e)$ can be obtained, where I_{max} and I_{min} are the moment of inertias corresponding to the cases $f_{E,S} = f_{min}$ and $f_{E,S} = f_{max}$, respectively. A number of additional limits germane to EBF then follows.

To have maximum energy dissipation in the link beam, short links yielding in shear are preferred over longer links yielding in flexure. The criterion for choosing a shear link length e (Engelhardt and Popov 1989) is

$$e \leq 1.6 \frac{M_p}{V_p} \tag{12}$$

where M_P and V_P = plastic moment and shear capacity of the link beam, respectively. Eq. (12) can be converted to a form suitable for the proposed design approach. Taking $M_P = M_{Pr} = Z'F_y$ and that $V_P = 0.58A_S F_y$ gives

$$e \leq \frac{1.6Z' \cdot F_y}{0.58A_S \cdot F_y} = \frac{2.77r \cdot Z}{A_S} = \frac{2.77r \cdot d(A_f + A_S/4)}{A_S} \tag{13}$$

where Z = plastic modulus of the entire section; Z' = reduced plastic modulus of the section to account for shear-moment interaction; and r = ratio of Z'/Z, a value that does not vary much and is always less than unity (it can be taken as 0.8 for preliminary design). Rearranging to solve for d, gives

$$d \geq d_3 \tag{14}$$

where

$$d_3 = \frac{e \cdot A_S}{2.77r(A_f + A_S/4)}$$

Another important design parameter that controls the ductile performance of EBF is the distortion angle of the link beam γ. From simple plastic analysis, for an eccentrically braced

frame of chevron bracing configuration, this link beam distortion angle is

$$\gamma = \frac{\Delta \cdot b}{e \cdot h} \tag{15}$$

where Δ = sway-displacement of the panel under consideration. The current consensus [*Manual* 1992; Canadian Standard Association (CSA) 1994] is that, for short links, this distortion should be limited to a γ_{max} equal to 0.09 rad. The minimum link length needed to comply with this code-permitted maximum distortion angle is therefore

$$e \geq \frac{\Delta \cdot b}{\gamma_{max} \cdot h} \tag{16}$$

Seismically induced displacement Δ can be predicted using an inelastic design spectrum, such as the Newmark-Hall spectrum adopted here for simplicity. For structures having a lateral fundamental period of vibration that falls within the constant velocity range of the spectrum, the maximum displacements obtained considering inelastic and elastic responses can be assumed to be nearly equal. Thus, for a given constant pseudovelocity PSv, mass M, and period T

$$\Delta = \frac{PSv}{\omega} = PSv \times \sqrt{\frac{M}{K_{Global}}} = PSv \times \sqrt{\frac{M}{\alpha}} \times \sqrt{f_{E,S}} \tag{17}$$

Combining (16) and (17) gives

$$e \geq \frac{PSvb}{h\gamma_{max}} \sqrt{\frac{M}{\alpha}} \times \sqrt{f_{E,S}} \tag{18}$$

Rearranging the preceding equation gives

$$f_{E,S} \leq \frac{\alpha}{M} \left(\frac{h\gamma_{max}}{PSvb} \right)^2 \times e^2 \tag{19}$$

Thus, another limit for the moment of inertia of the link beam I is obtained by combining (19) and (10)

$$I \geq I_0 \tag{20}$$

where

$$I_0 = \frac{\dfrac{h^2}{2b}\left(\dfrac{(a+e)^2}{3} - \dfrac{(b^2-2a^2)}{6}\right)}{\dfrac{\alpha}{M}\left(\dfrac{h\gamma_{max}}{PSvb}\right)^2 \times e^2 - \dfrac{(a^2+h^2)^{3/2}}{2A_b a^2} - \dfrac{h^3}{2A_{col}a^2} - \dfrac{(b-e)}{4A_l} - \dfrac{Eeh^2}{2GA_S ab}}$$

Using (11), this can be converted into another limit on beam depth d expressed as

$$d_4 = \sqrt{\frac{12I_0}{6A_f + A_S}} \tag{21}$$

Finally, slenderness of the beam web should be limited to prevent its buckling prior to large hysteretic energy dissipation. Hence, according to AISC (1992):

$$\frac{d}{t_w} \leq \frac{1{,}365}{\sqrt{F_y}} \tag{22}$$

Rearranging, to solve for d, gives

$$d \leq \frac{1{,}365}{\sqrt{F_y}} \times t_w \tag{23}$$

Then, multiplying both sides by d, substituting $d \cdot t_w = A_S$ and solving for d gives

$$d \leq d_5 \tag{24}$$

where

$$d_5 = \sqrt{\frac{1{,}365}{\sqrt{F_y}} \times A_S}$$

The preceding design constraints can be plotted as set of boundary curves, d_1 to d_5, as a function of end panel link eccentricity. A typical region bounded by all of those curves is shown in Fig. 1. Note this this zone of acceptable solutions may not exist or may be too small to comfortably account for design uncertainties. However, in such a case, the graphical tool makes it possible to identify, from the magnitude of the various terms involved in each constraint line, which design parameter could be changed with the most benefits. Once a region of valid solutions appears, theoretically, any point in that region is valid. However, points away from the borders are preferred to account for practical variations and tolerances likely to exist in the actual panel.

Once a satisfactory link length e^* and depth d^* are selected for the end ductile panels (as schematically shown in Fig. 1), the flexibility of the eccentrically braced panel [as in (8)] must be calculated. This makes it possible to calculate the required flexibility of the lower load path, as in (6) and to proceed with the design of the lower end ductile panels. Again, the required shear area of the link beam is given by (9) but now using the geometry of the lower end panel. Eqs. (10) and (11) can again be used to express the link depth d as a function of the link eccentricity e [i.e., $d(e)$]. In this case, however, a chosen solution (i.e., d^* and e^*) must lie on the line defined by (11), because flexibility of the lower load path is constrained to be proportional to that of the upper load path by (6).

Other constraints to the link beam used in the lower end panels are given by (14), (16), and (24), using geometry and panel displacements germane to the lower end panel (i.e., $\Delta_{L,E}$ instead of Δ). However, in this case, the limit on the link length imposed to comply with the specified maximum-permitted link distortion [(16)] can be calculated directly because the displacement $\Delta_{L,E}$ of the lower end panel can be determined directly from the known overall flexibility of the truss. Using the models derived in Sarraf and Bruneau (1998)

$$\Delta_{L,E} = \Delta - R_{L,E} \times f^* \tag{25}$$

where Δ is given by (17). The result of (16) can be directly plotted as a vertical line showing the minimum permissible link length e_{min}. Fig. 2 schematically shows how constraints on the depth of the lower end panel ductile link can be graphically presented as a function of link eccentricity, with a chosen satisfactory design given by d^* and e^*.

Note that due to its large number of constraints, and the fact that the yielding eccentric link is part of a beam whose stiffness has an important impact on the total panel stiffness, the EBF solution is probably the most difficult to design of the three ductile systems considered in this study. Systems for which the stiffness of the ductile device is decoupled from that of the lower beam are easier to design, as shown later.

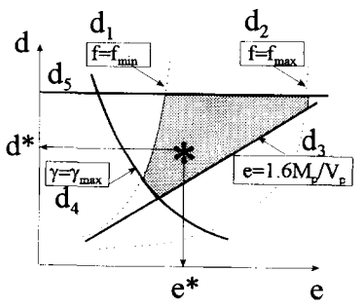

FIG. 1. Typical Region of Solution Bounded by Constraint Condition Curves for Design of EBF Link in End Panel of Deck-Truss Bridges

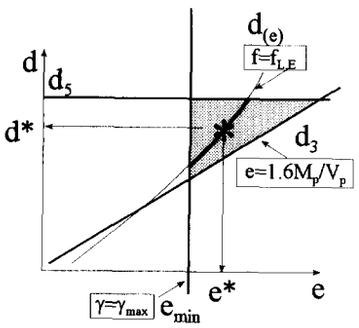

FIG. 2. Typical Solution Curve for Design of EBF in Lower End Panel of Deck-Truss Bridges

EBF Panel Design Example

The 80-m-span deck-truss considered by Sarraf and Bruneau (1998) has panel sizes of 10 m × 10 m, a total mass M of 640,000 kg, and a flexibility of the lower laterals sway-frame subsystem f^* of 2.1×10^{-8} m/N. It is assumed that yield capacities of $R_{E,S}$ = 1,023 kN and $R_{L,E}$ = 476 kN for the end panel and lower end panel, respectively, are required to protect the substructure and superstructure members of this truss. This gives a flexibility ratio $\alpha = 2 \times (1 + 476 \text{ kN}/1{,}023 \text{ kN}) = 2.94$. Following the procedure presented in Sarraf and Bruneau (1998), it is assumed that the structure fundamental lateral period of vibration must remain between T_{max} = 0.8 s and T_{min} = 0.48 s. Using those values in (3), the range for the flexibility of the end panel is delimited by 2.68×10^{-8} m/N $\leq f_{E,S} \leq 7.44 \times 10^{-8}$ m/N, which also satisfies the condition for the minimum flexibility as in (7) (i.e., $f_{E,S} \geq 9.87 \times 10^{-9}$ m/N).

The ductile end panel is first designed. Using the existing structure and geometry, b = 10 m, h = 10 m, $A_{col} = 10.3 \times 10^{-3}$ m^2, F_y = 300 MPa for the new ductile device, and $R_{E,S}$ = 1,023 kN, (9) gives a required link beam web shear area A_S of 5.88×10^{-3} m^2. Assuming a preliminary link length e of 1.5 m, braces are $(4.25^2 + 10^2)^{0.5} = 10.8$ m long. According to capacity design principles, braces are designed to remain elastic up to 1.5 times the shear link yield strength. A W310×202 (S.I. designation) having $A_b = 25.8 \times 10^{-3}$ m^2, C_r = 2,060 kN [according to CSA (1994)] is chosen to resist a factored compressive force of $C_f = 1{,}023 \times 1.5 \times (1/2) \times 10.8/4.25 = 1{,}966$ kN.

Knowing that the maximum permissible depth of the link beam [from (24)] is 0.681 m, a preliminary value for the flange area can easily be found by rearranging (13) and solving for A_f. For example, assuming a reduction factor r of 0.8, and a link beam depth of 0.5 m, $A_f = A_S(e/(2.77 \times r \cdot d) - 0.25) = 4.89 \times 10^{-3} \approx 5 \times 10^{-3}$ m^2. From the plot of the resulting constraint curves for this example [Fig. 3(a)], it is shown that the solution pair (e = 1.5, d = 0.5) does not fall in the admissible region. Adjustment of the preliminary values is thus necessary to move these curves and expand the zone of valid solutions. In this case, it is found that an increase of 20% in flange area (i.e., making $A_f = 6 \times 10^{-3}$ m^2) is sufficient with the new solution pair (e = 1.4, d = 0.6) falling well within the desirable range [Fig. 3(b)]. For this beam depth, and the required specified web shear area, the corresponding web thickness w can be calculated as $A_S/(d - 2 \times t_f) = 5.88 \times 10^{-3}$ m^2/0.6 m = 9.8 mm. Flange plates must be sized to comply with a specified width-to-thickness ratio limit, e.g., for $A_f = 6 \times 10^{-3}$ m^2, and $b_f/2t_f \leq 145/\sqrt{F_y} = 8.4$, select b_f = 300 and t_f = 20 mm. Flexibility of the retrofitted end panel from (8) becomes $f_{E,S} = 3.032 \times 10^{-8}$ m/N.

For that value, and α = 2.94, design of the ductile lower end panel can proceed as follows. Eqs. (6) and (5) give $f_{L,E} = 4.35 \times 10^{-8}$ m/N. For $R_{L,E}$ = 476 kN, (9) gives a required shear area for link beam of $A_S = 2.76 \times 10^{-3}$ m^2, for which

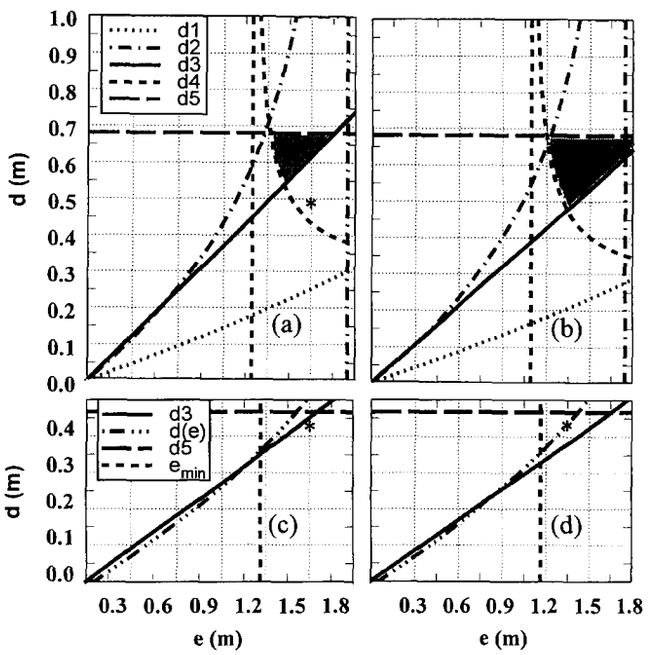

FIG. 3. Solution Curve for Example EBF End Panel: (a) First Trial; (b) Final Solution; and Lower End Panel: (c) First Trail; (d) Final Solution

(24) gives a maximum link beam depth d_{max} of 0.47 m. Eq. (17) gives Δ = 0.115 m, from which (25) can be used to calculate $\Delta_{L,E} = 0.115 - (476 \times 10^3)(2.1 \times 10^{-8}) = 0.105$ m. For that predicted displacement, (16) gives $e \geq 1.16$ m. Using a trial value of e = 1.5 m, a W310×107 brace (C_r = 1,036 kN and $A_b = 13.6 \times 10^{-3}$ m^2) is selected to elastically resist a calculated C_f = 913 kN. Assuming d = 0.45 m (≤0.47), a strength reduction factor r = 0.8, a link length e = 1.5 m (≥1.16), and rearranging (14) to find a trial value for the flange area gives: $A_f = 3.46 \times 10^{-3}$ m^2. Plotting the constraint curves in this case shows that the selected pair (e, d) does not fall within the admissible part of the curve [Fig. 3(c)]. However, selecting instead a $A_f = 3.52 \times 10^{-3}$ m^2 gives r = 0.84 and the satisfactory solution pair of d = 0.43 m and e = 1.35 m [Fig. 3(d)]. The resulting link beam has b_f = 220 mm, t_f = 16 mm, w = 6.35 mm. Note that the shorter link results in a longer brace, but the W310×107 previously selected brace is still satisfactory.

DESIGN OF VSL DUCTILE PANELS

Flexibility of VSL Panels

The flexibility $f_{E,S}$ of a ductile VSL panel can be expressed by the following equation:

$$f_{E,S} = \frac{b(s + d/2)^2}{12EI} + \frac{2((h - s - d/2)^2 + b^2/4)^{3/2}}{EA_b b^2} + \frac{2h(h - s - d/2)^2}{EA_{col} b^2} + \frac{b}{4EA_l} + \frac{s}{A_S G} \quad (26)$$

where s = height of the shear panel; I = bottom beam moment of inertia; and d = depth of the bottom beam. The other parameters are as previously defined following (8).

In this case, the inertia of the bottom beam I and the height of the vertical link s have the greatest impact on the flexibility of the ductile panel (in comparison with other parameters), and they are therefore chosen as the main design parameters. Rearranging (26) to express it in terms of the moment of inertia I gives

$$I = \frac{b(s + d/2)^2}{12\left\{Ef_{E,S} - \frac{2[(h - s - d/2)^2 + b^2/4]^{3/2}}{A_b b^2} - \frac{2h(h - s - d/2)^2}{A_{col} b^2} - \frac{b}{4A_l} - \frac{Es}{GA_S}\right\}} \tag{27}$$

Proposed Design Procedure

As was done for the EBF ductile panels, general constraints on the VSL panel must be expressed in terms of chosen design parameters, namely, I and s here. Thus, using the maximum and minimum permissible values of flexibility $f_{E,S}$ for this structure, (27) can be used to plot two constraint curves, $I_1 = (f_{max}, s)$ and $I_2 = (f_{min}, s)$. This is possible because h, b, A_{col}, and A_S are known—the latter value obtained by dividing the yield capacity of the panel by the steel shear yield strength, i.e., $A_S = R/(0.58F_y)$. The area of the bracing members A_b can be determined by designing the member for 1.5 times the compression force corresponding to the yield force of the VSL panel and calculating the brace length based on a preliminary assumption for the link length s. Initial values for A_l and d are estimated by determining the size of the bottom beam needed to elastically resist 1.5 times the moment applied at midspan when the VSL panel yields. Obviously, these values must be updated as the VSL dimensions change in subsequent design iterations.

Similarly to the EBF case, the shear distortion angle γ for short VSL links must not exceed a maximum distortion angle γ_{max} of 0.09 rad. From the geometry of plastic collapse mechanism of the VSL panel, $\gamma = \Delta/s$ and therefore

$$\frac{\Delta}{s} \le \gamma_{max} \quad \text{or} \quad \frac{\Delta}{\gamma_{max}} \le s \tag{28a,b}$$

The displacement response Δ can be predicted using (17), which, when substituted into (28), gives the following constraint on flexibility:

$$f_{E,S} \le \frac{\alpha}{M}\left(\frac{\gamma_{max}}{PSv}\right)^2 \times s^2 \tag{29}$$

Subsequently combining (27) with (29) gives

$$I \ge I_3 \tag{30}$$

where

$$I_3 = b(s + d/2)^2 \Bigg/ \left(12\left\{\frac{E\alpha}{M}\left(\frac{\gamma_{max}}{PSv}\right)^2 \times s^2 - \frac{2[(h - s - d/2)^2 + b^2/4]^{3/2}}{A_b b^2} - \frac{2h(h - s - d/2)^2}{A_{col} b^2} - \frac{b}{4A_l} - \frac{Es}{GA_S}\right\}\right)$$

The preceding design constraint can be plotted as a function of vertical link length. A typical region of admissible solution, bounded by the curves defined by the preceding equations for I_1, I_2, and I_3 curves, is shown in Fig. 4. As explained earlier, points away from the borders are preferred. Furthermore, the bottom beam must also be able to elastically resist 1.5 times the moment applied by the link, which translates into the following constraint on its elastic modules S_b:

$$S_b \ge \frac{1.5R \times (s + d/2)}{2F_y} \tag{31}$$

Finally, shear yielding of the VSL is preferred over flexural yielding. Thus, using an equation analogous to (12), but recognizing that moment is zero at the top of the VSL, the following constraint on the size of the link must also be satisfied:

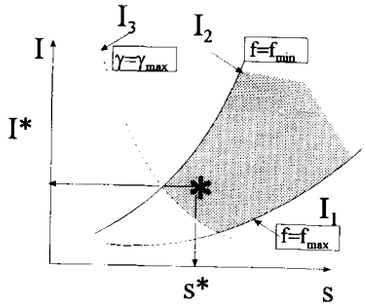

FIG. 4. Typical Region of Solution Bounded by Constraint Condition Curves for Design of VSL Link in End Panel of Deck-Truss Bridges

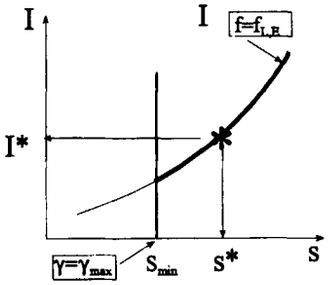

FIG. 5. Typical Solution Curve for Design of VSL Link in Lower End Panel of Deck-Truss Bridges

$$s \le \frac{0.8M_P}{V_P} \quad \text{or} \quad Z \ge \frac{1.25s \cdot V_P}{F_y} \tag{32a,b}$$

where V_P = yield capacity in shear for the link beam, which can be taken as equal to yield capacity of the panel R. Other design requirements such as width-to-thickness ratio limits for web and flanges of shear link [i.e., (22)] and bottom beam, must also be satisfied, but these dimensions can be adjusted as necessary for given values of I and s.

To proceed with the design of the lower end ductile panel, once satisfactory VSL height s^*, VSL moment of inertia I^*, and bottom beam dimensions are selected, flexibility of the lower load path $f_{L,S}$ and of the lower end panel $f_{L,E}$ are calculated using (6) and (5), respectively. Subsequently, replacing $f_{E,S}$ by $f_{L,E}$, in (27), the bottom beam moment of inertia I becomes a function of link height s, i.e., any selected pair (i.e., I^* and s^*) must lie on the curve defined by (27). Finally, as in (28), only points with $s \ge s_{min}$ are admissible along the curve, where s_{min} is the minimum link length for which the VSL distortion angle reaches its maximum limit (i.e., $\gamma = \gamma_{max}$), when $\Delta = \Delta_{max}$ [see (25) and (28)]. Fig. 5 shows a typical I-s curve and its zone of admissible solutions.

Design Example on VSL

The same 80-m-span deck-truss described earlier is again used here, and it is constrained to the same range of admissible periods and flexibilities for end panel as those calculated for the EBF example.

The ductile end panel is first designed. Here again, $F_y = 300$ MPa for the ductile device, $R_{E,S} = 1{,}023$ kN, and (9) gives a required vertical link shear area A_S of 5.88×10^{-3} m^2. Assuming a preliminary link height $s = 1.0$ m gives a brace length of 11.22 m. For $F_y = 350$ MPa, an HSS 305×305×11 (S.I. designation) brace having $A_b = 12.8 \times 10^{-13}$ m^2 and $C_r = 1{,}856$ kN [according to CSA (1994)] is adequate to resist the factored compressive force resulting from 1.5 times the vertical link shear yield strength ($C_f = 1{,}023$ kN × 1.5 × (1/2) × 11.22/5 = 1,721 kN). A E610×101 bottom beam, having $A_l = 13 \times 10^{-3}$ m^2 and $d = 0.608$ m, can elastically resist the moment induced by the link.

As shown in Fig. 6(a), constraint curves I_1, I_2, and I_3 can be plotted, which corresponds to the minimum and maximum values of $f_{E,S}$ = 2.68 × 10^{-8} m/N and 7.44 × 10^{-8} m/N, and γ_{max} = 0.09 rad. Link length must be at least 1.2 m or greater, regardless of the value of moment of inertia for the bottom beam. Note that selecting very high values of s may not be advantageous, as it will increase the required moment capacity of the bottom beam. Moreover, due to the shape of the admissible region of solution (at the left corner), choosing values of s very close to the minimum value of 1.2 requires high values of moment of inertia, resulting in a very heavy beam. Choosing a reasonable link length of 1.3 m, the new brace member length and force become $L_b = (8.7^2 + 5^2)^{0.5}$ = 10.03 m, and C_f = 1,023 kN × 1.5 × (1/2) × 10.03/5 = 1,539 kN. A HSS 305×305×9.5 having A_b = 11 × 10^{-3} m^2, and C_r = 1,850 kN is selected. The minimum elastic modulus of the bottom beam [from (31)] is $S_{x,min} = 1.5P$. $S/2F_y$ = (1,023 kN × 1.3 m × 1.5)/(2 × 300 MPa × 10^6) = 3.324 × 10^{-3} m^3. The new resulting constraint curves are shown in Fig. 6(b), with an acceptable range for the moment of inertia of the bottom beam of 700 × 10^6 mm^4 < I < 1,200 × 10^6 mm^4 when s = 1.3 m. A W460×193 (A_l = 24.6 × 10^{-3} m^2, I = 1,020 × 10^6 mm^4, S_x = 4.19 × 10^{-3} m^3) is selected to satisfy constraints on both S_x and I. The limit on the web width-to-thickness ratio is then used to find the maximum permitted depth of the vertical link. Assuming t_w = 9 mm, the required depth of the link web is d = 5.88 × 10^{-3} m^2/9 mm = 653.3 mm, which is less than d_{max} = 680 mm [24)]. Subsequently, the size of the flanges is determined to provide sufficient moment capacity. Eq. (32) gives $Z \geq$ 5.541 × 10^6 mm^3, which for the known web dimension translates into a minimum required flange area of A_f = 7.013 × 10^{-3} m^2. For this minimum area, respecting the width-to-thickness ratio limit of the flange, t_f = 2 mm and b_f = 320 mm are chosen, which gives Z = 5.711 × 10^6 mm^3 and I_S = 1.814 × 10^9. It is noteworthy that the contribution of flexural flexibility of the link beams to total panel deflection is negligible when short links are used, and (26) or (27) were derived accordingly. However, once the size of the vertical link and bottom beam sections are known, the additional flexibility term $s^3/3EI_S$ can be added to (26) to give a more accurate

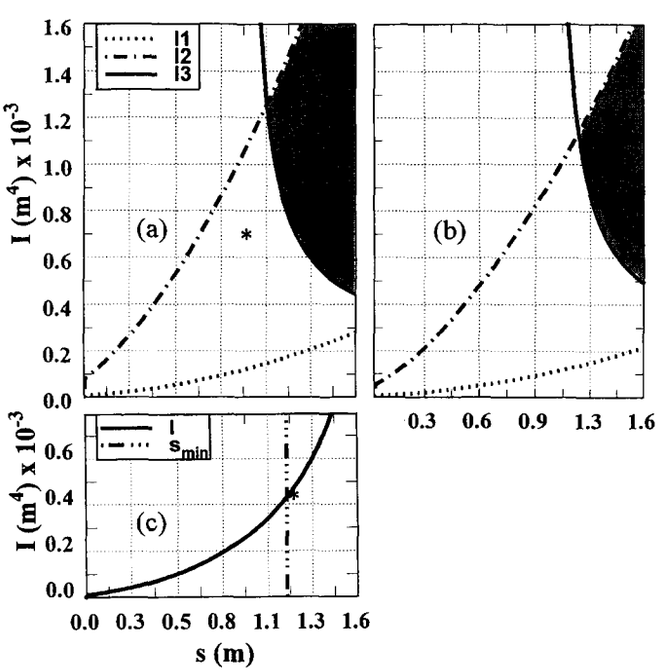

FIG. 6. Solution Curve for Example VSL End Panel: (a) First Trial; (b) Final Solution; and Lower End Panel: (c) First Trial; (d) Final Solution

value for panel flexibility which results in $f_{E,S}$ of 3.704 × 10^{-8} m/N instead of 3.502 × 10^{-8} m/N (a 5.4% difference).

Knowing f^* = 2..1 × 10^{-8} m/N (from the companion paper), design of the ductile lower end panel can proceed as follows. Using (5) and (6) gives $f_{L,S}$ = 6.532 × 10^{-8} and $f_{L,E}$ = 4.432 × 10^{-8}. For $R_{L,E}$ = 476 kN, the shear area required for the vertical link is A_S = 2.76 × 10^{-3} m^2. Eq. (17) gives Δ = 0.1,164 m, from which (25) can be used to calculate $\Delta_{L,E}$ = 0.1064 m. For this predicted drift value, and considering γ_{max} = 9%, (28) gives $s \geq$ 1.18 m. Using a trial value of s = 1.2 m, an HSS 203×203×11 (C_r = 750 kN and A_b = 8.23 × 10^{-3} m^2) is selected to elastically resist a calculated C_f = 722 kN. For A_c = 42 × 10^{-3} m^2, b = 10 m, and h = 10 m, the inertia curve for the specified flexibility $f_{L,E}$ can be plotted [Fig. 6(c)]. From here onward, design proceeds following exactly the same steps as for the preceding end panel case. Thus, for s = 1.2 m, I = 4.5 × 10^{-4}, and (31) (with an estimated d = 0.5 m) gives $S_b \geq$ 1.73 × 10^{-3} (m^3). A W460×97 (A = 1.23 × 10^{-2} m^2, d = 0.466, S_b = 1.91 × 10^{-3} m^3, and I = 4.5 × 10^{-4} m^3) is selected that satisfies both conditions for I and S_b. The shear link web thickness t_w = 6 mm and its link beam depth d_S = 2,767/6 = 0.461 m ≤ d_{max} = 0.466 m [(24)]. From (32), $Z \geq$ 2.38 × 10^{-3} m^3, t_f = 24 mm, and b_f = 187.8 mm are selected, resulting in Z = 2.396 × 10^{-3} m^3. Moment of inertia of the link beam is I_S = 5.79 × 10^{-4} m^4, and the flexibility of the lower end panel, including the effect of flexural flexibility of the shear link, is $f_{L,E}$ = 4.44 × 10^{-8} m/N, as desired.

DESIGN OF TADAS DUCTILE PANELS

Flexibility of TADAS Panels

Unlike the EBF and VSL systems, the distortion angle of a TADAS device is not necessarily related to its ductility demand. The flexible triangular plates used in TADAS devices yield in flexure and can be designed to provide a large deformation capability at only moderate levels of inelastic deformations. The design constraint on distortion angle, which is only relevant for devices yielding in shear (e.g., the EBF and VSL systems), is therefore not imposed here.

Generally, it is uneconomical and inefficient to design TADAS systems to have a high stiffness. As will be subsequently demonstrated, for a given TADAS yield strength and plate height, regardless of the number of plates used, the required plate thickness increases proportionally to the required stiffness. Thus, economy steers design toward greater flexibility, and only the upper limit on flexibility (from the second section of this paper) needs to be considered. Besides, given that TADAS systems dissipate hysteretic energy by bending steel plates, they are highly ductile and the lower limit on flexibility adopted in this study would be too stringent for this type of systems. It is usally sufficient to simply check that the expected ductility demands for the final design are reasonable and within the capabilities reported for this type of systems (Tsai et al. 1993). This lesser number of constraints compared to the EBF and VSL systems make the TADAS systems relatively easier to design.

The required flexibility of the triangular plates alone, expressed in terms of an admissible flexibility value of the end panel and other panel member properties, is given by

$$f_T = f_{E,S} - \left(\frac{b(\eta \cdot h + d/2)^2}{12EI} + \frac{2\{[(1-\eta)h - d/2]^2 + (b/2)^2\}^{3/2}}{EA_b b^2} + \frac{2h[(1-\eta)h - d/2]^2}{EA_{col} b^2} + \frac{b}{4EA_l} \right) \quad (33)$$

where η = ratio of the height of triangular plates-to-the height of the panel and other parameters correspond to the panel

members similar to those of VSL panel. Tsai et al. (1993) recommended using $\eta = 0.10$.

Proposed Design Procedure

Given that TADAS panel height does not change considerably during the design process, the bottom beam and braces can be designed first to elastically resist 1.5 times the panel yield force. The TADAS device itself is then designed to provide a panel strength R with a device flexibility of f_T. For a device having n triangular plates, each cantilever plate being subjected to tip load P^*

$$P^* \cdot u = m_p \quad \text{or} \quad \left(\frac{R}{n}\right) \cdot u = \frac{vt^2}{4} F_y \qquad (34a,b)$$

where u, v, and t = plate height, width, and thickness, respectively; and m_p = plastic moment of a triangular plate at its base. The flexibility of n triangular TADAS plates is (Tsai et al. 1993) as follows:

$$f_T = \frac{6u^3}{Envt^3} \qquad (35)$$

Eqs. (34) and (35) can be combined to give the plate height required for a given flexibility, panel strength, and plate thickness

$$u = \sqrt{t} \times \sqrt{\frac{2Ef_TR}{3F_y}} \qquad (36)$$

or the plate thickness required for a given flexibility, panel strength, and plate height

$$t = \frac{3u^2F_y}{2Ef_TR} \qquad (37)$$

The number of TADAS plates needed, n, is given by (34) rearranged as follows:

$$n = \frac{4\beta R}{F_y t^2} \qquad (38)$$

where $\beta = u/v$ = plate aspect ratio. Fig. 7(a) shows schematically how n varies as a function of plate thickness t for a given β. For β^* chosen without the recommended limits of 1.5–3, a small integer value for n^* can be chosen, with a corresponding plate thickness t^* (geometry β^* can be adjusted slightly to accommodate available plate thickness sizes). From these selected properties, (35) is used to calculate the actual f_T^*, which is generally smaller than the target f_T.

Having values of $f_{E,S}$ and f^*, design of the ductile lower end panel can proceed as done for the other systems; i.e., actual value for end panel flexibility is determined, and, for a known ratio α, (6) and (5) are used to determine the lower end panel flexibility target $f_{L,E}$. Design then proceeds using (33)–(38), as earlier, with the exception that $f_{E,S}$ is replaced by $f_{L,E}$ in (33).

TADAS Panels Design Example

The same 80-m-span deck-truss bridge used previously is considered. However, design here is controlled by drift limit of the panel, and the initial design value for end panel flexibility is taken as $f_{E,S} = f_{max} = 8.4 \times 10^{-8}$ m/N.

The ductile end panel is first designed. Using the recommended value of $\eta = 0.1$, for panel height $h = 10$ m, the TADAS height u of 1 m is selected, which gives a brace length of $(9^2 + 5^2)^{0.5} = 10.29$ m. According to capacity design principle, W310×158 braces ($A_b = 20.1 \times 10^{-3}$ m^2, $C_r = 1{,}728$ kN) are selected to resist a compressive force of $C_f = 1{,}023 \times 1.5 \times (1/2) \times 10.29/5 = 1{,}579$ kN. As for the bottom beam, assuming $d = 0.6$ m and $F_y = 350$ MPa, (31) gives a minimum required elastic modulus $S_b \geq (1{,}023 \text{ kN} \times 1.3 \text{ m} \times 1.5)/(2 \times 350 \text{ MPa} \times 10^6) = 2.85 \times 10^{-3}$ m^3. A W610×113 ($A = 14.4 \times 10^{-3}$ m^2, $S = 2.88 \times 10^{-3}$ m^3, and $I = 8.75 \times 10^{-4}$ m^4) is selected.

For the chosen braces and bottom beam, (33) gives $f_T = 6.27 \times 10^{-8}$ m/N. For $F_y = 300$ MPa, (37) gives a required TADAS plate thickness t of 35 mm. Choosing a typical value of $\beta = 2$ for the plate aspect ratio, (38) indicates that 22 triangular plates are required. A smaller number of plates is desirable, and (38) [Fig. 7(b)] is used to find a satisfactory final design: $\beta = 2.0$, $n^* = 14$, and $t^* = 44$ mm, for panel dimensions $u = 1.0$ m and $v = 0.5$ m. The corresponding flexibilities are then calculated to be $f_T^* = 5.01 \times 10^{-8}$ m/N [(35)] and $f_{E,S} = 7.14 \times 10^{-8}$ m/N [(33)], which are below the upper limit of $f_{max} = 8.4 \times 10^{-8}$ m/N.

For design of the ductile lower end panel, geometry is identical, and $\eta = 0.1$ again gives $u = 1$ m and a brace length of 10.29 m. A W310 ×107 brace ($A_b = 13.6 \times 10^{-3}$ m^2, $C_r = 1{,}132$ kN) is adequate to resist a $C_f = 476 \times 1.5 \times (1/2) \times 10.29/5 = 735$ kN, and a W460×74 lower beam ($A = 9.45 \times 10^{-3}$ m^2, $S_x = 1.46 \times 10^{-3}$ m^3, and $I = 333 \times 10^{-6}$ m^4) provides the needed $S_b \geq 1.43 \times 10^{-3}$ m^3 for an assumed $d = 0.4$ m. Using the same flexibility ratio α as in the previous examples, (5) and (6) give $f_{L,S} = 1.52 \times 10^{-7}$ m/N and $f_{L,E} = 1.3 \times 10^{-7}$ m/N. The required flexibility for the TADAS plates [(33)] is $f_T = 1.01 \times 10^{-7}$ m/N, and (37) gives a required plate thickness $t = 46.2$ mm. For $\beta = 2.0$, (38) gives a corresponding number of plates $n = 5.9$. Some adjustments are obviously

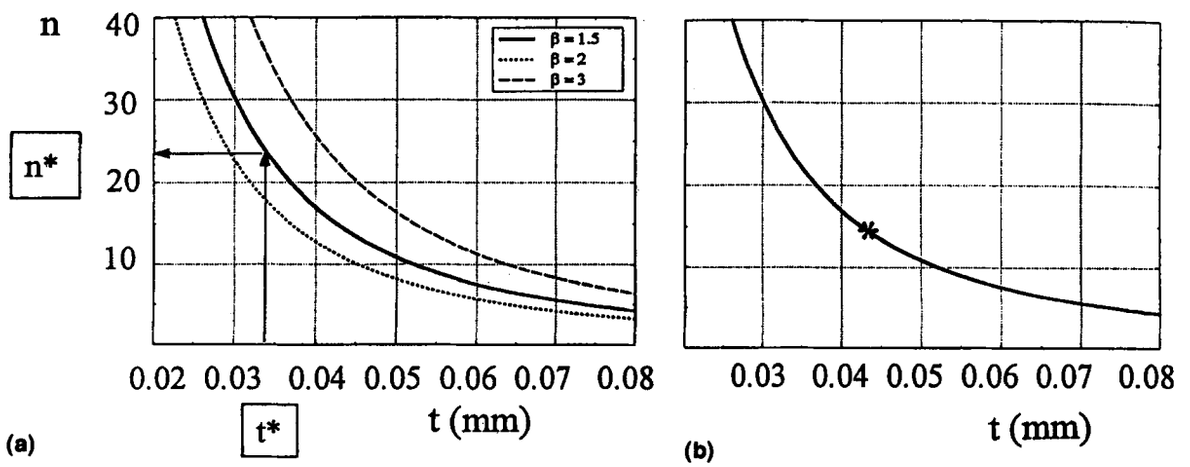

FIG. 7. Number of TADAS Plates as Function of Thicknesses: (a) Typical Curves $F_y = 300$ MPa and Overall Yield Capacity $R = 1{,}023$ kN; (b) Final Solution for $\beta = 2.0$

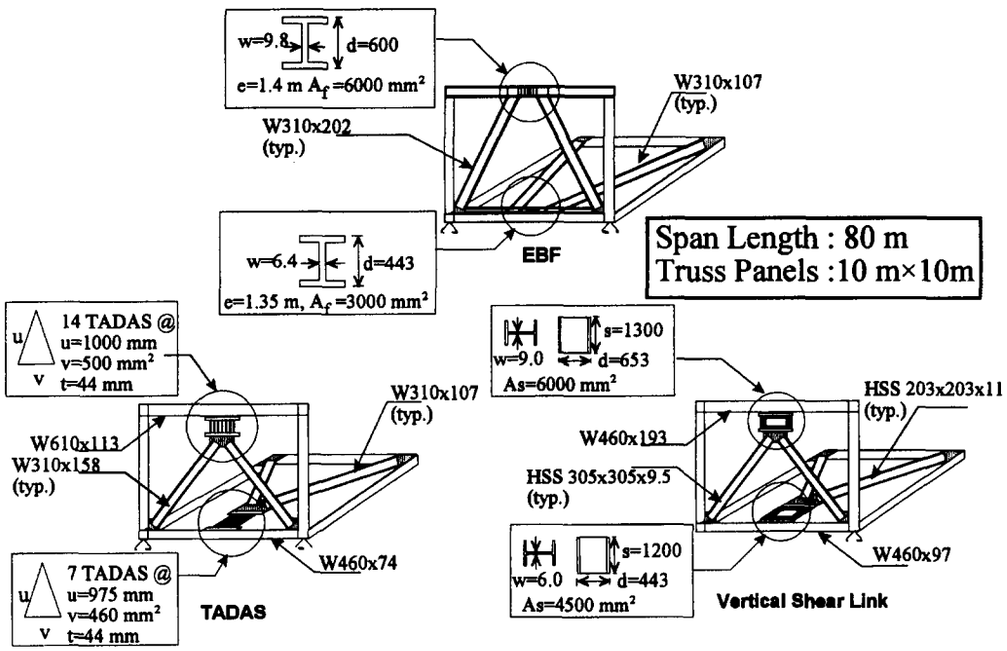

FIG. 8. Details of Ductile Retrofit Design for EBF, VSL, and TADAS Systems for Example Deck-Truss Bridge

necessary. Selecting an available plate thickness t^* of 44 mm (i.e., same as that of the end panel), (38) indicates that 6.6 plates are required. Rounding this number to $n^* = 7$, β becomes 2.12. Geometry of the TADAS is modified accordingly, to $u = 0.975$ m and $v = 0.460$ m.

The final TADAS system design is shown in Fig. 8, along with the corresponding designs for the other two ductile systems considered in this study.

DYNAMIC ANALYSES OF RETROFITTED TRUSS

Computer models of the three retrofitted trusses were generated to conduct dynamic nonlinear inelastic analyses using the DRAIN-3DX software (Prakash et al. 1994). The truss members were modeled using a simple bilinear element with elastic buckling in compression and plastic yielding in tension. Bottom beams in the ductile panels were modeled using flexural members that allowed local plastic hinges. Each EBF link beam was modeled using a combination of elastic flexural members, multilinear inelastic flexural plastic hinges, and multilinear inelastic end shear connections, with postyield stiffnesses set to simulate strain hardening in shear or flexure. Each TADAS device was modeled using a single prismatic cantilever calibrated to have the proper strength and stiffness, coupled with multiple moment connections at its base to simulate moment plastic hinging with postyielding nonlinear strain hardening. Each VSL was modeled as a vertical cantilever with a nonlinear inelastic connection at its base to simulate yielding in shear.

Ground acceleration records from the El Centro 1940, Northridge 1994, San Fernando 1971 (Pacoma Dam), Loma Prieta 1989, Olympia 1949 and Taft 1952 earthquakes were selected for the time-history analyses. These are representative of western U.S. seismicity. If these records were scaled to a $0.4g$ maximum peak ground acceleration (the maximum value in AASHTO's current seismic maps), the average response spectrum for these six records would compare reasonably well with the Newmark-Hall design spectrum constructed for a peak ground acceleration of $0.4g$. However, in this study, the selected ground acceleration records were scaled such that their average elastic response spectrum would nearly match the Newmark-Hall mean-plus-one-standard-deviation elastic design spectrum for a peak ground acceleration of $0.4g$ (i.e., the design basis for the ductile retrofits).

Distortion angle of yielding elements, overall drift, and ductility ratios obtained from the time-history analyses are presented in Table 1, in terms of average and maximum values obtained for the six earthquakes considered. Note that for a particular excitation, the value of distortion angle or drift may not necessarily be smaller than their corresponding limits; however, the average values are well within the design expectations, and the retrofits are deemed to perform satisfactorily.

Of the six scaled earthquake records, the El Centro was scaled to $0.6g$ and caused the largest shear distortion in the VSL system. The time-history analysis of this distortion angle is plotted in Fig. 9, with two horizontal lines that represent the threshold of yielding. This gives a qualitative indication of the number of yield excursions and cumulative ductility demands. Two cycles had large local ductility demands, up to ~11, most

TABLE 1. Average Displacement and Maximum Ductility Response to Six Earthquakes[a]

Ductile retrofit system (1)	Distortion angle γ (%) (2)	Maximum distortion angle γ (%) (3)	Average global ductility demand μ (4)	μ_{max} (5)	Average end panel drift (%) (6)	Maximum drift (%) (7)	All requirements satisfied (8)
EBF	2.6	9	2.68	3.75	0.54	2	√
TADAS	—[b]	—[b]	2.34	3.75	1.59	2	√
VSL	2.99	9	2.57	3.75	0.75	2	√

[a]Scaled to $\mu + \sigma$ Newmark-Hall design spectra for peak ground acceleration of $0.4g$ and damping of 2% checked against their permissible limits.
[b]Not applicable.

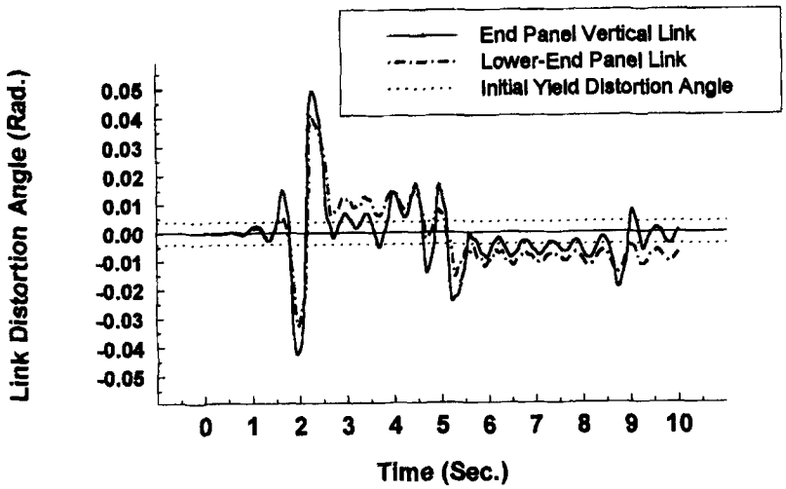

FIG. 9. Nonlinear Time-History Response for Link Distortion Angle γ of Both End and Lower End Panels in Deck-Truss Retrofitted Using VSL

other inelastic cycles being less than half that value. This local ductility is within reported capacities for shear yielding systems (Malley and Popov 1983).

CONCLUSIONS

Deck-truss bridges can be retrofitted by converting the end cross-frames and lower end panels adjacent to the truss supports into special ductile panels acting as structural fuses. However, given the complex behavior of deck-truss bridges subjected to earthquakes, the design of such retrofitted systems must respect constraints on flexibilities to limit global drifts and ductility demands, as well as other constraints germane to the type of ductile device introduced. In this paper, a systematic design procedure is proposed to take into account all of those constraints that control the dynamic response of ductile retrofitted deck-truss bridges. A graphical approach is presented and shown to be an effective way to rapidly steer the design toward a satisfactory solution. This design tool is also used to show why some solutions exist for certain ductile device properties, and how to enlarge the range of possible solutions.

Example retrofit of an 80-m-span deck-truss bridge was accomplished successively using EBF, VSL, and TADAS devices into the special ductile panels. This showed how to tailor the general design approach to account for the specific features of given ductile devices. TADAS systems are found to be subjected to less constraints than the EBF and VSL systems and are thus relatively simpler to design. Nonlinear inelastic three-dimensional time-history analyses were performed for the resulting retrofitted bridges subjected to six earthquakes scaled so that their average spectrum matched the mean-plus-one-standard-deviation Newmark-Hall spectrum for $0.4g$ ground acceleration. Results show that the proposed design procedure is adequate to ensure the satisfactory ductile seismic performance of the retrofitted systems.

APPENDIX. REFERENCES

Bouwkamp, J. G., Tamajani, N. G., Schneither, B., and Kakalagos, A. (1994). "Design of an eccentrically-braced test frame with vertical shear links." *Proc., 2nd Int. Conf. on Earthquake Resistant Constr. and Des.*

Bruneau, M., Uang, C. M., and Whittaker, A. (1997). *Ductile design of steel structures.* McGrawHill Inc., New York, N.Y.

Canadian Standard Association (CSA). (1994). "Limit states of steel structures." *Rep. No. CAN/CSA-S16.1-M94*, Rexdale, Ontario, Canada.

Engelhardt, M. D., and Popov, E. P. (1989). "On the design of eccentrically braced frames." *Earthquake Spectra*, 5(3), 495–511.

Fehling, E., Pauli, W., and Bouwkamp, J. G. (1992). "Use of vertical shear-links in eccentrically braced frames." *Proc., 10th World Conf. on Earthquake Engrg.*, Vol. 8, A. A. Balkema, Rotterdam, The Netherlands, 4475–4479.

Malley, J. O., and Popov, E. P. (1983). "Design considerations for shear links in eccentrically braced frames." *Rep. No. UCB/EERC-83/24*, Earthquake Engrg. Res. Ctr., Univ. of California, Berkeley, Calif.

Manual of steel construction (LRFD). 2nd Ed., American Institute for Steel Construction, Chicago, Ill.

Nakashima, M. (1994). "Energy dissipation behavior of shear panels made of low yield steel." *Earthquake Engrg. and Struct. Dyn.*, 23(12), 1299–1313.

Prakash, V., Powell, G. H., and Campbell, S. (1994). "DRAIN-3DX base program description and user guide." *Rep. No. UCB/SEMM-94/07*, Dept. of Civ. Engrg., Univ. of California, Berkeley, Calif.

Roeder, C. W., and Popov, E. P. (1977). "Inelastic behavior of eccentrically braced steel frames under cyclic loadings." *Rep. No. UCB/EERC-77/18*, Earthquake Engrg. Res. Ctr., Univ. of California, Berkeley, Calif.

Sarraf, M., and Bruneau, M. (1998). "Ductile seismic retrofit of steel deck-truss bridges. I: Strategy and Modeling." *J. Struct. Engrg.*, ASCE, 124(11), 1253–1262.

Tsai, K.-C., Chen, H.-W., Hong, C.-P., and Su, Y.-F. (1993). "Design of steel triangular plate energy absorbers for seismic-resistant construction." *Earthquake Spectra*, 9(3), 505–528.